



BENDING MOMENT INFLUENCE SURFACES FOR RECTANGULAR CONCRETE PLATES SIMPLY SUPPORTED AT THREE EDGES AND BUILT-IN AT THE FOURTH EDGE

Sabah S. Razouki

Prof. of Civil Engineering College of Engineering, Nahrain University, Baghdad-Iraq.

Zena R. Al-Ani

Assistant Lecturer in Civil Engineering, College of Engineering, Nahrain University, Baghdad-Iraq.

ABSTRACT

Presented in this paper is a series of bending moment influence surfaces for concrete rectangular plates simply supported at three edges and built-in at the fourth edge. The solutions are obtained analytically on the basis of thin plate's theory with small deflection using double Fourier series. The influence surfaces are presented for two observation points namely the center of the plate as well as the midpoint of the built-in edge. A computer program was written in FORTRAN language to generate the influence surfaces making use of the developed analytical solutions of this work. The validity of the computer solution was confirmed by comparing its results with published results for zero Poisson's ratio and excellent agreement was obtained. An application of the influence surfaces for the case of a line load as well as a strip load is also presented.

The paper reveals that the bending moment influence surfaces depend on the actual value of Poisson's ratio, aspect ratio of the plate, and position of the observation point.

الخلاصة

يقدم هذا البحث حلولاً تحليلية لسطوح التأثير لعزوم الانحناء لألواح كونكريتية مستطيلة بسيطة الاسناد في ثلاثة حافات ومبنية في حافتها الرابعة اعتماداً على نظرية الألواح النحيفة ذات الأود القليل. أن سطوح التأثير التي تم تطويرها في هذا البحث، قد خصصت لأيجاد عزوم الانحناء في نقطتين من نقاط الملاحظة: الأولى في مركز اللوح والثانية في نقطة الوسط للحافة المبنية.

لقد تم كتابة برنامج على الحاسبة بلغة الفورتران لغرض إيجاد سطوح الانحناء وذلك بالاعتماد على الحلول التحليلية التي تم تطويرها في هذا البحث.

أظهرت مقارنة النتائج للحلول التحليلية التي طورت في هذا العمل توافقاً ممتازاً مع نتائج حلول متوفرة لنسبة بوسون تساوي صفر.

ان البحث يبين بأن سطوح التأثير لعزوم الانحناء تعتمد على نسبة بوسون والنسبة بين أبعاد اللوح (الطول/العرض) و موقع نقاط الملاحظة.

KEYWORDS: aspect ratio, bending moment, influence surfaces, plates, Poisson's ratio.

INTRODUCTION

For bridge decks, the types of construction are divided into beam, grid, slab, beam and slab, and cellular. A slab deck behaves like a flat plate which is structurally continuous for the transfer of moments and torsions in all directions within the plane of the plate (**Hambly, 1976**).

In bridge design, the most important and most difficult task faced by the structural designer is the accurate estimation of the loads, which may be applied to a structure during its life. After loads are estimated the next problem is to decide the worst possible combinations of these loads which might occur at one time (**McCormac, 1989**). The concept of considering an actual bridge deck as an equivalent plate for the purpose of determining the distribution of stresses is well established (**Cusens and Pama, 1975**).

Influence lines can be used for two very important purposes (**Merritt, 1999**); the first purpose is, to determine what position of live loads will lead to a maximum value of the particular function for which an influence line has been constructed. The second purpose is the value of that function with the load so placed or, in fact, for any loading condition.

The influence surface represents a two-dimensional analogue of the one-dimensional influence lines. They are independent of the mode of loading and can be evaluated easily for each load case, for plane structures which are indispensable for the analysis of bridge structures (**Pucher, 1973**).

Pucher (1973) obtained influence surfaces for the internal forces of various plates but they are restricted to Poisson's ratio equal to zero with length to width ratio equal to 0.8, 1.0, and 1.2.

Timoshenko and Woinowsky –Krieger (1989) presented analytical results for the bending moments of rectangular plates with various edge conditions and a Poisson's ratio of 0.3.

Razouki and Al-Lami (2005) studied the effect of Poisson's ratio on the bending moment influence surfaces for simply supported rectangular plates. Also **Razouki and AL-Ani (2006)** studied the effect of Poisson's ratio on the bending moment influence surfaces for rectangular plates simply supported at two parallel edges and fixity at the other opposite edges.

It is worth mentioning that the software **LARSA** can deal with influence surfaces of plate-deck models using standard and new two-dimensional vehicle definitions that model both the length and width of the vehicle and tire contact area.



Finally, it is useful to note that **Boyd et.al (1999) and Wang et.al (2000)** made use of the influence surface theory of thin plate for representing mathematically the human knee joint surfaces.

POISSON'S RATIO:

The Poisson's ratio of concrete is a basic function in analyzing and designing prestressed and ordinary reinforced concrete plates and shells (**Klink, 1985**).

Francis et.al. (1991) stated that Poisson's ratio was found to be insensitive to the age and the richness of concrete mix and may be taken as approximately 0.19 for concrete. According to **ACI Committee 363 (1984)**, the value for Poisson's ratio of light weight aggregate high strength concrete is equal to 0.2 and for normal weight high strength concretes, Poisson's ratio varies between 0.2 and 0.28.

According to **Kupfer and Gerstle (1973)**, Poisson's ratio for concrete shows some dependency on the stress ratios. They obtained a value of 0.2 for biaxial compression, 0.18 for biaxial tension and a range of 0.18 to 0.2 for tension compression state of stress. **Neville and Brooks (1987)** pointed out that Poisson's ratio for concrete has been observed to remain approximately constant up to a stress level of 80% of the concrete strength. Beyond this level, Poisson's ratio increases rapidly and values in excess of 1.0 have been measured by **Darwing and Pecknold (1977)**. **Mirza et.al (1979)** reported that Poisson's ratio under uniaxial tension is somewhat lower than in uniaxial compression. For the purpose of analysis in this work, the value of Poisson's ratio to be considered for concrete is 0.2. However, the analysis remains valid for any other material having a Poisson's ratio close to that for concrete.

KIRCHHOFF-LOVE THEORY OF THIN PLATES :

Timoshenko and Woinowsky –Krieger (1989) differentiate between thin plate theory with small deflection and that for large deflection.

However, **Zehender et.al (1998)** reported that the crack tip stress field in a plate described in terms of the small deflection Kirchhoff plate theory is still valid for large deflections.

Thus , the use of thin plate with small deflection is quite justified.

According to **Szilard (1974)**, the small deflection plate theory which is attributed to Kirchhoff and Love, is governed by the following differential equation describing the behavior of isotropic plate which was obtained by Lagrange in 1811 (**Timoshenko and Woinowsky –Krieger , 1989**)

$$\frac{\partial^4 w}{\partial x^4} + 2 \frac{\partial^4 w}{\partial x^2 \partial y^2} + \frac{\partial^4 w}{\partial y^4} = \frac{q(x, y)}{D} \quad (1)$$

where

w = lateral displacement of the plate.

q(x, y) = intensity of lateral load.

D = flexural rigidity of the plate.

$$D = \frac{Eh^3}{12(1-\nu^2)} \quad (2)$$

E = modulus of elasticity of the plate material.

h = plate thickness.

ν = Poisson's ratio of the plate material.

The bending and twisting moments can be obtained in terms of deflection surface as follows

(Timoshenko and Woinowsky –Krieger,1989):

$$\left. \begin{aligned} M_x &= -D \left(\frac{\partial^2 w}{\partial x^2} + \nu \frac{\partial^2 w}{\partial y^2} \right) \\ M_y &= -D \left(\frac{\partial^2 w}{\partial y^2} + \nu \frac{\partial^2 w}{\partial x^2} \right) \\ M_{xy} &= -M_{yx} = D(1-\nu) \frac{\partial^2 w}{\partial x \partial y} \end{aligned} \right\} \quad (3)$$

where

M_x = bending moment per unit length acting on the sections parallel to the y- axis.

M_y = bending moment per unit length acting on the sections parallel to the x- axis.

M_{xy}, M_{yx} = Twisting moment per unit length of sections perpendicular to the x and y axes respectively.

According to **Timoshenko and Woinowsky-Krieger (1989)**, the analytical solution for rectangular plates simply supported at three edges and built-in at the fourth edge as shown in Fig.1 can be determined by superposition approach .This approach makes use of Navier solution and Levy solution for simply supported plate at all four edges as discussed below.

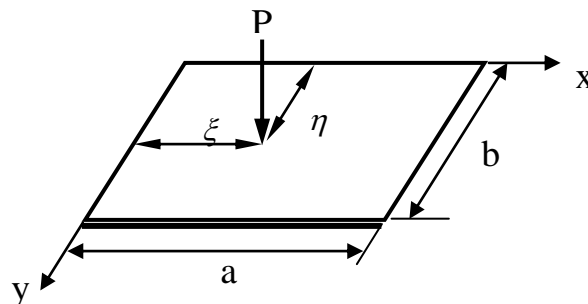


Fig.1 point load on the plate.

BENDING MOMENTS FOR RECTANGULAR LOADED AREA ON THE PLATES:

Various methods of solution of the plate equation are available (**Girkmann 1963; Szilard 1974 and Taylor and Govindjee 2002**). However, the double Fourier series is adopted in this work as it ensures convergence.

For a simply supported rectangular plate at four edges subjected to rectangular loaded area as shown in Fig.2, **Timoshenko and Woinowsky-Krieger (1989)** stated that the deflected surface $w_1(x, y)$ is

$$w_1(x, y) = \frac{16q_0}{\pi^6 D} \sum_{m=1}^{\infty} \sum_{n=1}^{\infty} \frac{\sin \frac{m\pi\xi}{a} \sin \frac{n\pi\eta}{b} \sin \frac{m\pi u}{2a} \sin \frac{n\pi v}{2b} \sin \frac{m\pi x}{a} \sin \frac{n\pi y}{b}}{mn \left[\frac{m^2}{a^2} + \frac{n^2}{b^2} \right]^2} \tag{4}$$

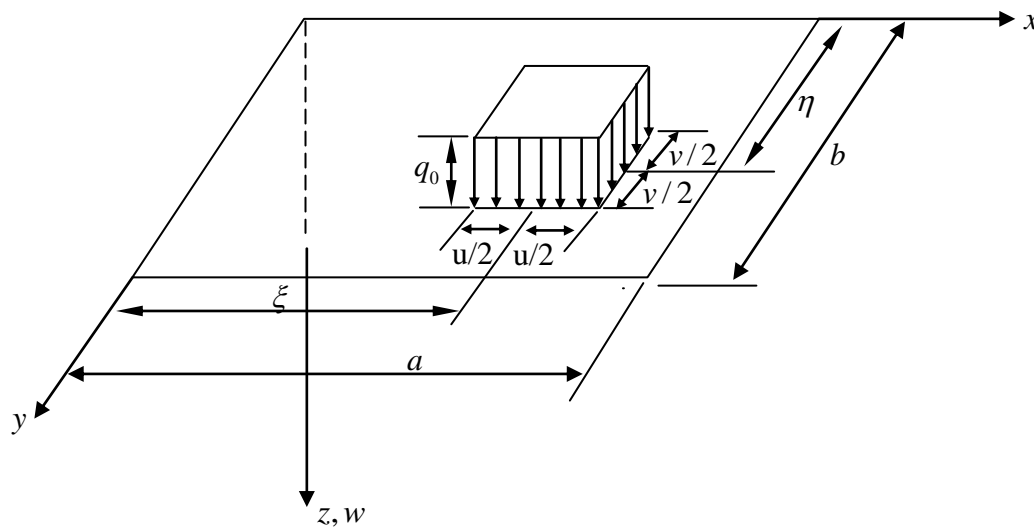


Fig.2 simply supported rectangular plate with uniform loading on a rectangular area

a = the length of built-in edge.

b = the dimension of the plate perpendicular to built-in edge.

The deflected surface for a simply supported rectangular plate subjected to distributed moment at the edge $y_2=b/2$ as shown in Fig.3 becomes (**Timoshenko and Woinowsky-Krieger, 1989**):

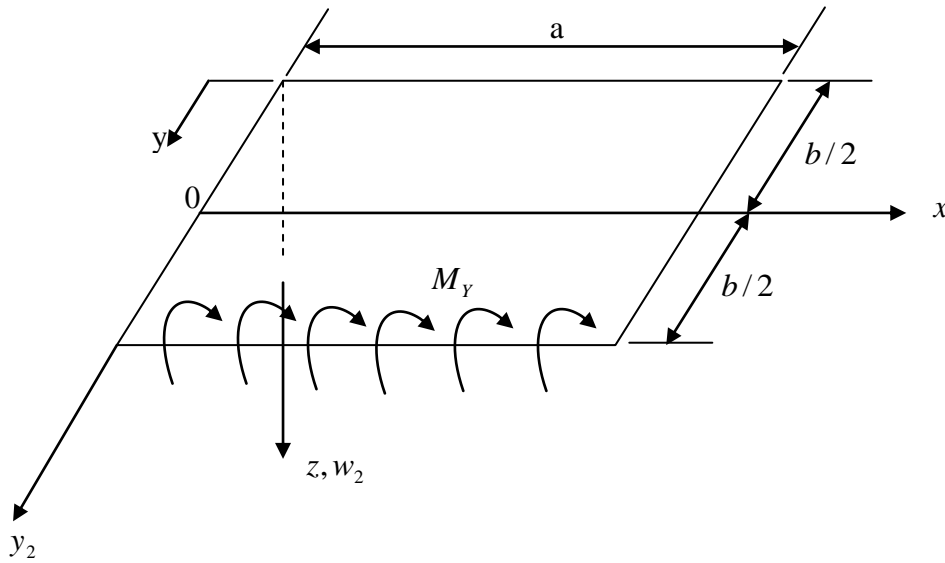


Fig.3 distributed moment at the built-in edge $y_2 = b/2$ after Szilard (1974)

$$w_2(x, y) = \frac{a^2}{4\pi^2 D} \sum_{m=1}^{\infty} \frac{E_m \sin \frac{m\pi x}{a}}{m^2} \left[\frac{1}{\cosh \alpha_m} \left(\alpha_m \tanh \alpha_m \cosh \frac{m\pi y_2}{a} - \frac{m\pi y_2}{a} \sinh \frac{m\pi y_2}{a} \right) + \frac{1}{\sinh \alpha_m} \left(\alpha_m \coth \alpha_m \sinh \frac{m\pi y_2}{a} - \frac{m\pi y_2}{a} \cosh \frac{m\pi y_2}{a} \right) \right] \quad (5)$$

where

$$y_2 = y - b/2$$

$$\alpha_m = \frac{m\pi b}{2a} \quad (6)$$

E_m = coefficients of a single sine series of distributed moment at the edge $y_2 = b/2$

The parameter E_m can be determined by using the condition at built-in edge which indicates that the two slopes are equal in magnitude and of opposite signs.

This means

$$\left(\frac{\partial w_1}{\partial y} \right)_{(x, y=b)} = - \left(\frac{\partial w_2}{\partial y_2} \right)_{(x, y_2=b/2)} \quad (7)$$

The slope $\frac{\partial w_1}{\partial y}$ produced by rectangular loaded area can be determined from Eq.(4) as follows :

$$\left(\frac{\partial w_1}{\partial y} \right)_{y=b} = \frac{16q_0}{\pi^5 b D} \sum_{m=1}^{\infty} \sum_{n=1}^{\infty} \frac{\sin \frac{m\pi \xi}{a} \sin \frac{n\pi \eta}{b} \sin \frac{m\pi u}{2a} \sin \frac{n\pi v}{2b} \sin \frac{m\pi x}{a} \cos n\pi}{m \left[\frac{m^2}{a^2} + \frac{n^2}{b^2} \right]^2}$$

The distributed moment M_y at the side $y_2=b/2$ shown in Fig.2 produces the following slope from Eq.(5):

$$\left(\frac{\partial w_2}{\partial y_2}\right)_{y_2=b/2} = \frac{a}{4\pi D} \sum_{m=1}^{\infty} \frac{E_m \sin \frac{m\pi x}{a}}{m} \left[\frac{1}{\cosh \alpha_m} \left(\alpha_m \tanh \alpha_m \sinh \frac{m\pi b}{2a} - \sinh \frac{m\pi b}{2a} - \frac{m\pi b}{2a} \cosh \frac{m\pi b}{2a} \right) + \frac{1}{\sinh \alpha_m} \left(\alpha_m \coth \alpha_m \cosh \frac{m\pi b}{2a} - \cosh \frac{m\pi b}{2a} - \frac{m\pi b}{2a} \sinh \frac{m\pi b}{2a} \right) \right]$$

where { see Eq.(6) }

$$\alpha_m = \frac{m\pi b}{2a}$$

The substitution into above equation yields

$$\left(\frac{\partial w_2}{\partial y_2}\right)_{y_2=b/2} = \frac{a}{4\pi D} \sum_{m=1}^{\infty} \frac{E_m \sin \frac{m\pi x}{a}}{m} (\alpha_m \tanh^2 \alpha_m - \tanh \alpha_m + \alpha_m \coth^2 \alpha_m - \coth \alpha_m - 2\alpha_m) \tag{8}$$

Then, E_m can be obtained from the condition of Eq.(7) as follows:

$$E_m = \frac{-64 q_0 a^3}{\pi^4 b} \sum_{n=1}^{\infty} \frac{\sin \frac{m\pi \xi}{a} \sin \frac{n\pi \eta}{b} \sin \frac{m\pi u}{2a} \sin \frac{n\pi v}{2b} \cos n\pi}{\left[m^2 + \frac{n^2 a^2}{b^2} \right]^2 (\alpha_m \tanh^2 \alpha_m - \tanh \alpha_m + \alpha_m \coth^2 \alpha_m - \coth \alpha_m - 2\alpha_m)} \tag{9}$$

or

$$E_m = \frac{-64 Pa^3}{\pi^4 buv} \sum_{n=1}^{\infty} \frac{\sin \frac{m\pi \xi}{a} \sin \frac{n\pi \eta}{b} \sin \frac{m\pi u}{2a} \sin \frac{n\pi v}{2b} \cos n\pi}{\left[m^2 + \frac{n^2 a^2}{b^2} \right]^2 (\alpha_m \tanh^2 \alpha_m - \tanh \alpha_m + \alpha_m \coth^2 \alpha_m - \coth \alpha_m - 2\alpha_m)} \tag{10}$$

Thus, the bending moments can be obtained as follows: { see Eq.(3) }

$$M_x = \frac{16 q_0 a^2}{\pi^4} \sum_{m=1}^{\infty} \sum_{n=1}^{\infty} \frac{\left[m^2 + \nu \frac{n^2 a^2}{b^2} \right] \sin \frac{m\pi \xi}{a} \sin \frac{n\pi \eta}{b} \sin \frac{m\pi u}{2a} \sin \frac{n\pi v}{2b} \sin \frac{m\pi x}{a} \sin \frac{n\pi y}{b}}{mn \left[m^2 + \frac{n^2 a^2}{b^2} \right]^2} + \frac{1}{4} \sum_{m=1}^{\infty} E_m \sin \frac{m\pi x}{a} \left[\frac{1}{\cosh \alpha_m} \left\{ (1-\nu) \left(\alpha_m \tanh \alpha_m \cosh \frac{m\pi y_2}{a} - \frac{m\pi y_2}{a} \sinh \frac{m\pi y_2}{a} \right) + 2\nu \cosh \frac{m\pi y_2}{a} \right\} + \frac{1}{\sinh \alpha_m} \left\{ (1-\nu) \left(\alpha_m \coth \alpha_m \sinh \frac{m\pi y_2}{a} - \frac{m\pi y_2}{a} \cosh \frac{m\pi y_2}{a} \right) + 2\nu \sinh \frac{m\pi y_2}{a} \right\} \right] \tag{11}$$

$$M_Y = \frac{16q_0 a^2}{\pi^4} \sum_{m=1}^{\infty} \sum_{n=1}^{\infty} \left[\frac{\nu m^2 + \frac{n^2 a^2}{b^2}}{mn \left[m^2 + \frac{n^2 a^2}{b^2} \right]^2} \sin \frac{m\pi\xi}{a} \sin \frac{n\pi\eta}{b} \sin \frac{m\pi u}{2a} \sin \frac{n\pi v}{2b} \sin \frac{m\pi x}{a} \sin \frac{n\pi y}{b} \right. + \left. \frac{1}{4} \sum_{m=1}^{\infty} E_m \sin \frac{m\pi x}{a} \left[\frac{1}{\cosh \alpha_m} \left\{ (\nu - 1) \left(\alpha_m \tanh \alpha_m \cosh \frac{m\pi y_2}{a} - \frac{m\pi y_2}{a} \sinh \frac{m\pi y_2}{a} \right) + 2 \cosh \frac{m\pi y_2}{a} \right\} + \frac{1}{\sinh \alpha_m} \left\{ (\nu - 1) \left(\alpha_m \coth \alpha_m \sinh \frac{m\pi y_2}{a} - \frac{m\pi y_2}{a} \cosh \frac{m\pi y_2}{a} \right) + 2 \sinh \frac{m\pi y_2}{a} \right\} \right] \right] \quad (12)$$

To have a good check on the results obtained, use can be made of the case of full uniform loading over the whole plate treated by **Timoshenko and Woinowsky –Krieger (1989)** for which they presented the bending moments at the midpoint of the built-in edge and at the middle of the plate. For the case of full load $u=a$, $v=b$ and equations (11) and (12) give the dimensionless bending moments

$$m_x = \frac{M_x}{q_0 a^2} = \frac{16}{\pi^4} \sum_{m=1}^{\infty} \sum_{n=1}^{\infty} \left[\frac{m^2 + \nu \frac{n^2 a^2}{b^2}}{mn \left[m^2 + \frac{n^2 a^2}{b^2} \right]^2} \sin \frac{m\pi\xi}{a} \sin \frac{n\pi\eta}{b} \sin \frac{m\pi}{2} \sin \frac{n\pi}{2} \sin \frac{m\pi x}{a} \sin \frac{n\pi y}{b} \right. + \left. \frac{1}{4} \sum_{m=1}^{\infty} E_m^* \sin \frac{m\pi x}{a} \left[\frac{1}{\cosh \alpha_m} \left\{ (1 - \nu) \left(\alpha_m \tanh \alpha_m \cosh \frac{m\pi y_2}{a} - \frac{m\pi y_2}{a} \sinh \frac{m\pi y_2}{a} \right) + 2\nu \cosh \frac{m\pi y_2}{a} \right\} + \frac{1}{\sinh \alpha_m} \left\{ (1 - \nu) \left(\alpha_m \coth \alpha_m \sinh \frac{m\pi y_2}{a} - \frac{m\pi y_2}{a} \cosh \frac{m\pi y_2}{a} \right) + 2\nu \sinh \frac{m\pi y_2}{a} \right\} \right] \right] \quad (13)$$

$$m_y = \frac{M_Y}{q_0 a^2} = \frac{16}{\pi^4} \sum_{m=1}^{\infty} \sum_{n=1}^{\infty} \left[\frac{\nu m^2 + \frac{n^2 a^2}{b^2}}{mn \left[m^2 + \frac{n^2 a^2}{b^2} \right]^2} \sin \frac{m\pi\xi}{a} \sin \frac{n\pi\eta}{b} \sin \frac{m\pi}{2} \sin \frac{n\pi}{2} \sin \frac{m\pi x}{a} \sin \frac{n\pi y}{b} \right. + \left. \frac{1}{4} \sum_{m=1}^{\infty} E_m^* \sin \frac{m\pi x}{a} \left[\frac{1}{\cosh \alpha_m} \left\{ (\nu - 1) \left(\alpha_m \tanh \alpha_m \cosh \frac{m\pi y_2}{a} - \frac{m\pi y_2}{a} \sinh \frac{m\pi y_2}{a} \right) + 2 \cosh \frac{m\pi y_2}{a} \right\} + \frac{1}{\sinh \alpha_m} \left\{ (\nu - 1) \left(\alpha_m \coth \alpha_m \sinh \frac{m\pi y_2}{a} - \frac{m\pi y_2}{a} \cosh \frac{m\pi y_2}{a} \right) + 2 \sinh \frac{m\pi y_2}{a} \right\} \right] \right] \quad (14)$$

Arly Eq.(10) becomes

$$E_m^* = \frac{E_m}{q_0 a^2} = \frac{-64 a}{\pi^4 b} \sum_{n=1}^{\infty} \frac{\sin \frac{m\pi\xi}{a} \sin \frac{n\pi\eta}{b} \sin \frac{m\pi}{2} \sin \frac{n\pi}{2} \cos n\pi}{\left[m^2 + \frac{n^2 a^2}{b^2} \right]^2 \left(\alpha_m \tanh^2 \alpha_m - \tanh \alpha_m + \alpha_m \coth^2 \alpha_m - \coth \alpha_m - 2\alpha_m \right)} \tag{15}$$

BENDING MOMENTS FOR POINT LOAD ON THE PLATE:

For the case of a point load as shown in Fig.1 which is of interest for the generation of the influence surfaces, the coordinates ζ and η refer to the position of the point load, while those x and y refer to the position of the observation point and the value of E_m from Eq.(10) becomes :

$$E_m = \frac{-64 P a^3}{\pi^4 b} \lim_{\substack{u \rightarrow 0 \\ v \rightarrow 0}} \sum_{n=1}^{\infty} \frac{\sin \frac{m\pi\xi}{a} \sin \frac{n\pi\eta}{b} \sin \frac{m\pi u}{2a} \sin \frac{n\pi v}{2b} \cos n\pi}{uv \left[m^2 + \frac{n^2 a^2}{b^2} \right]^2 \left(\alpha_m \tanh^2 \alpha_m - \tanh \alpha_m + \alpha_m \coth^2 \alpha_m - \coth \alpha_m - 2\alpha_m \right)}$$

Noting that $\lim_{\substack{u \rightarrow 0 \\ v \rightarrow 0}} \sin \frac{m\pi u}{2a} \sin \frac{n\pi v}{2b} = \frac{mn\pi^2}{4ab}$ and by letting $P=1$, the above equation gives the dimensionless value of E_m

$$E_m^* = \frac{E_m b}{P a} = \frac{-16 a}{\pi^2 b} \sum_{n=1}^{\infty} \frac{mn \sin \frac{m\pi\xi}{a} \sin \frac{n\pi\eta}{b} \cos n\pi}{\left[m^2 + \frac{n^2 a^2}{b^2} \right]^2 \left(\alpha_m \tanh^2 \alpha_m - \tanh \alpha_m + \alpha_m \coth^2 \alpha_m - \coth \alpha_m - 2\alpha_m \right)} \tag{16}$$

Thus , the dimensionless bending moments m_x and m_y become:

$$m_x = \frac{M_x b}{a} = \frac{4}{\pi^2} \sum_{m=1}^{\infty} \sum_{n=1}^{\infty} \frac{\left[m^2 + v \frac{n^2 a^2}{b^2} \right] \sin \frac{m\pi\xi}{a} \sin \frac{n\pi\eta}{b} \sin \frac{m\pi x}{a} \sin \frac{n\pi y}{b}}{\left[m^2 + \frac{n^2 a^2}{b^2} \right]^2} + \left[\frac{1}{4} \sum_{m=1}^{\infty} E_m^* \sin \frac{m\pi x}{a} \left\{ \frac{1}{\cosh \alpha_m} \left\{ (1-\nu) \left(\alpha_m \tanh \alpha_m \cosh \frac{m\pi y_2}{a} - \frac{m\pi y_2}{a} \sinh \frac{m\pi y_2}{a} \right) + 2\nu \cosh \frac{m\pi y_2}{a} \right\} + \frac{1}{\sinh \alpha_m} \left\{ (1-\nu) \left(\alpha_m \coth \alpha_m \sinh \frac{m\pi y_2}{a} - \frac{m\pi y_2}{a} \cosh \frac{m\pi y_2}{a} \right) + 2\nu \sinh \frac{m\pi y_2}{a} \right\} \right\} \right] \tag{17}$$

$$m_y = \frac{M_y b}{a} = \frac{4}{\pi^2} \sum_{m=1}^{\infty} \sum_{n=1}^{\infty} \frac{\left[\nu m^2 + \frac{n^2 a^2}{b^2} \right] \sin \frac{m\pi\xi}{a} \sin \frac{n\pi\eta}{b} \sin \frac{m\pi x}{a} \sin \frac{n\pi y}{b}}{\left[m^2 + \frac{n^2 a^2}{b^2} \right]^2} + \left[\frac{1}{4} \sum_{m=1}^{\infty} E_m^* \sin \frac{m\pi x}{a} \left\{ (\nu-1) \left(\alpha_m \tanh \alpha_m \cosh \frac{m\pi y_2}{a} - \frac{m\pi y_2}{a} \sinh \frac{m\pi y_2}{a} \right) + 2 \cosh \frac{m\pi y_2}{a} \right\} + \frac{1}{\sinh \alpha_m} \left\{ (\nu-1) \left(\alpha_m \coth \alpha_m \sinh \frac{m\pi y_2}{a} - \frac{m\pi y_2}{a} \cosh \frac{m\pi y_2}{a} \right) + 2 \sinh \frac{m\pi y_2}{a} \right\} \right\} \right] \tag{18}$$

GENERATION OF INFLUENCE SURFACES:

All influence surfaces were generated by applying the unit load to numerous points of the plate and evaluating the particular effect of moment produced at the observation point. The development of the influence surfaces is achieved by using a computer program written in this work in FORTRAN language and a program (**Surfer**) for plotting the contour-lines.

To show the validity of the developed solution and the written computer program, a comparison with available solutions is made. The case of a square plate ($a/b=1.0$) having a Poisson's ratio equal to zero with the observation point at the center of the plate, has been chosen as the corresponding influence surface is available by **Pucher (1973)**.

Figure 4 shows that the contour lines obtained from the computer program are in excellent agreement with **Pucher's** solution.

To check the validity of the computer program dealing with the bending moment evaluation, the cases of rectangular plates with $a/b= 0.5, 1.0, 1.1, 1.2, 1.3, 1.4, 1.5$ and 2.0 subjected to uniform load over the whole plate and having a Poisson's ratio of 0.3 have been chosen. This is due to the fact that data for the bending moment at the center of built-in edge are available by **Timoshenko and Woinowsky-Krieger (1989)**. Figure 5 shows that the results of the bending moment m_y at the center of the built-in edge are in excellent agreement with those obtained by **Timoshenko and Woinowsky-Krieger (1989)**.

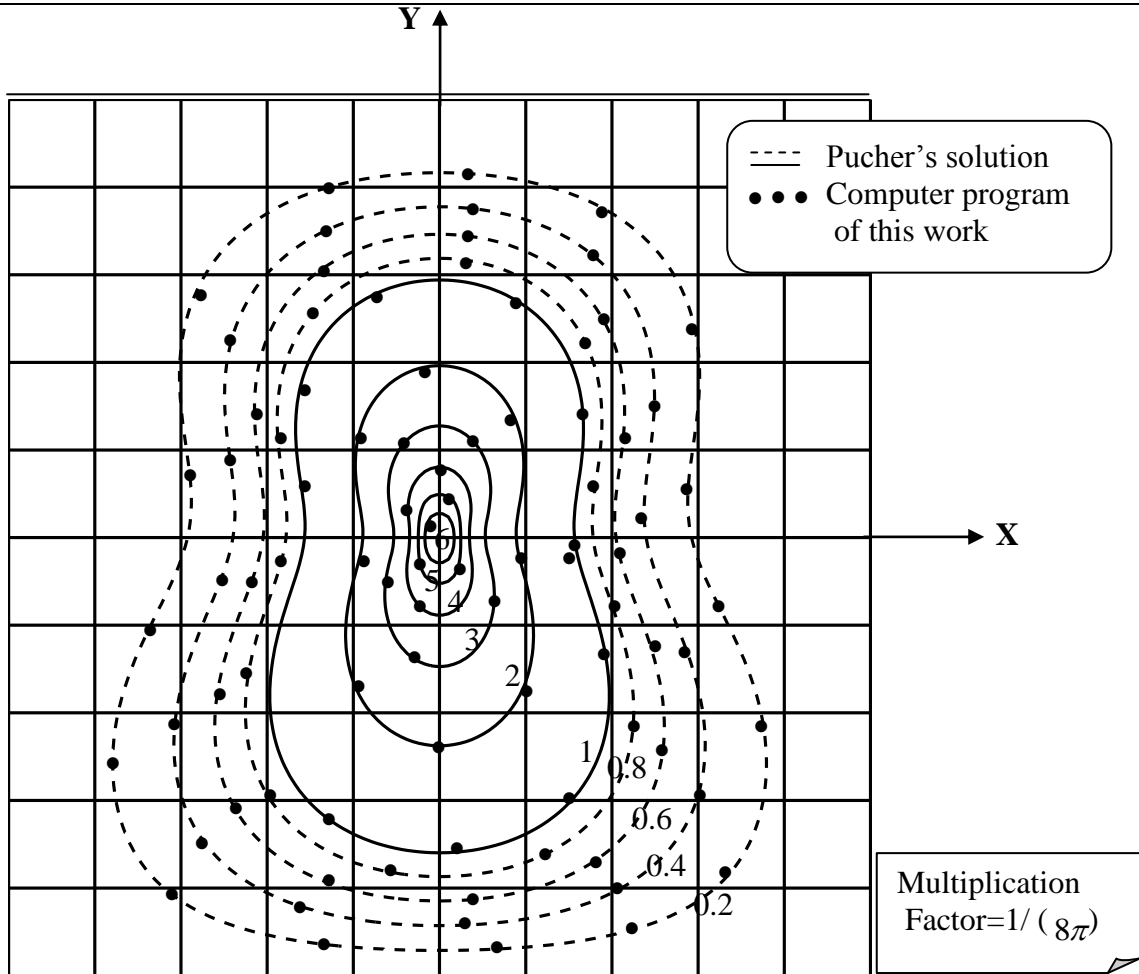


Fig.4 Comparison between the influence surface for m_x obtained from computer program with Pucher's (1973) solution for the center of a square plate having zero Poisson's ratio.

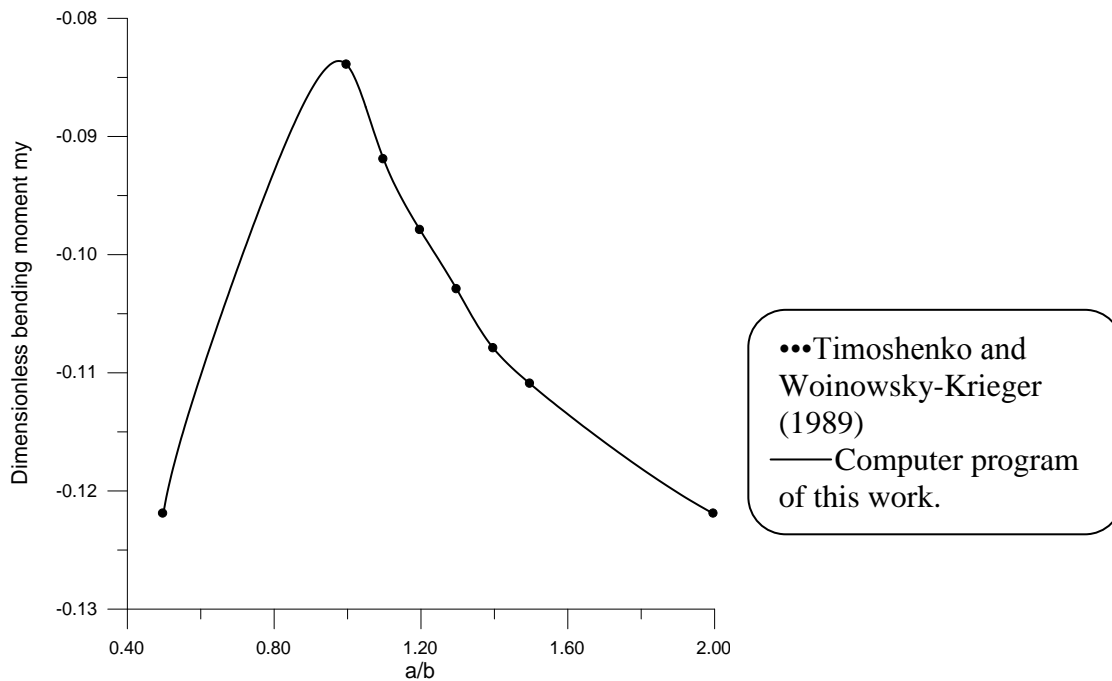


Fig.5 Comparison between Timoshenko and Woinowsky-Krieger(1989) and computer program for evaluation of bending moment m_y at the center of built-in edge of a rectangular plate with different values of aspect ratio a/b and having Poisson's ratio of 0.3

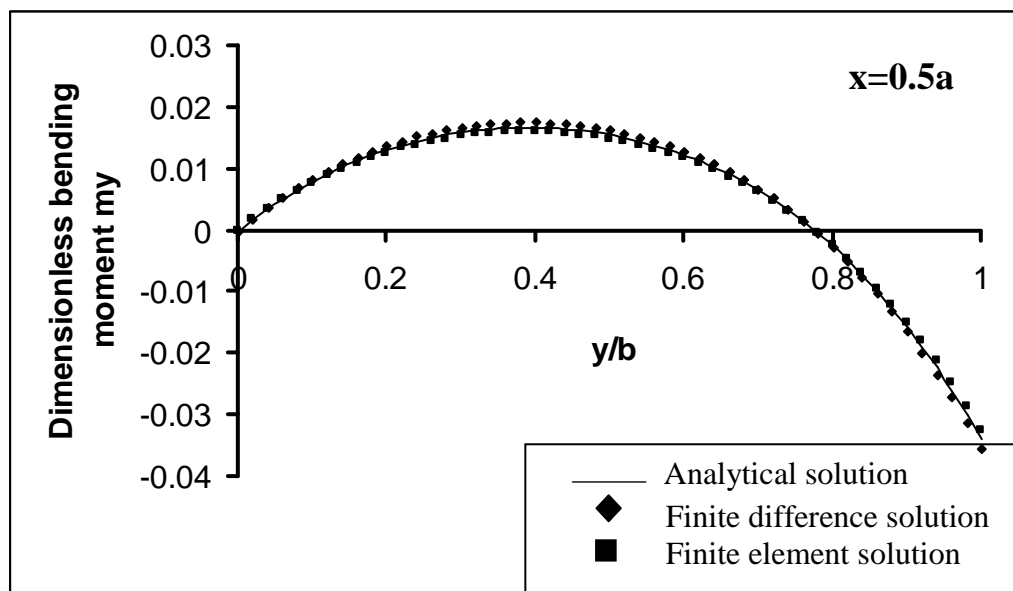
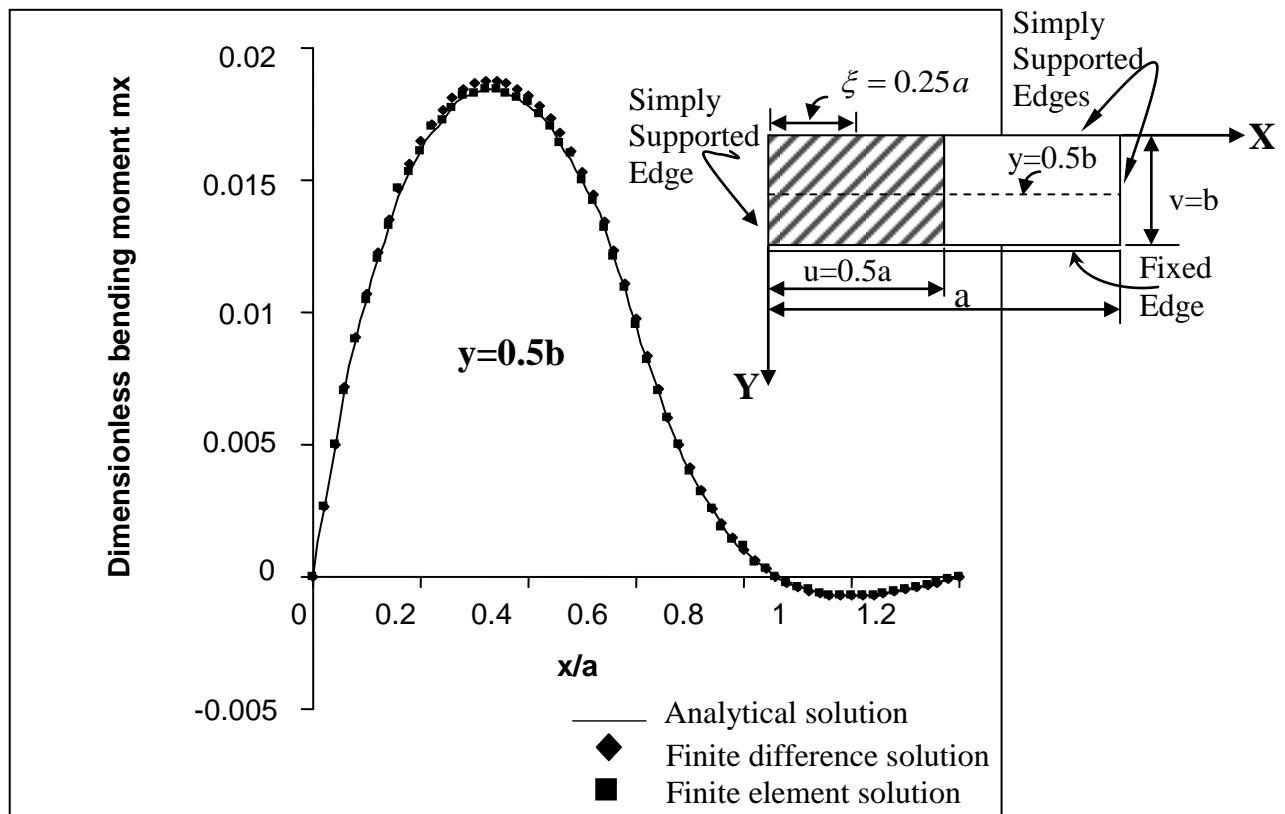


Fig.6 Comparison between analytical, finite difference and finite element solutions for bending moments m_x at $y=0.5b$ and m_y at $x=0.5a$ for a rectangular plate ($a/b=1.2$) with partial loading having Poisson's ratio of 0.2

Figures 7 to 13 present influence surfaces for rectangular plates simply supported at three edges and built-in at the four edge with aspect ratio a/b equal to 0.6, 1.0, 1.4 and 2.0 respectively.

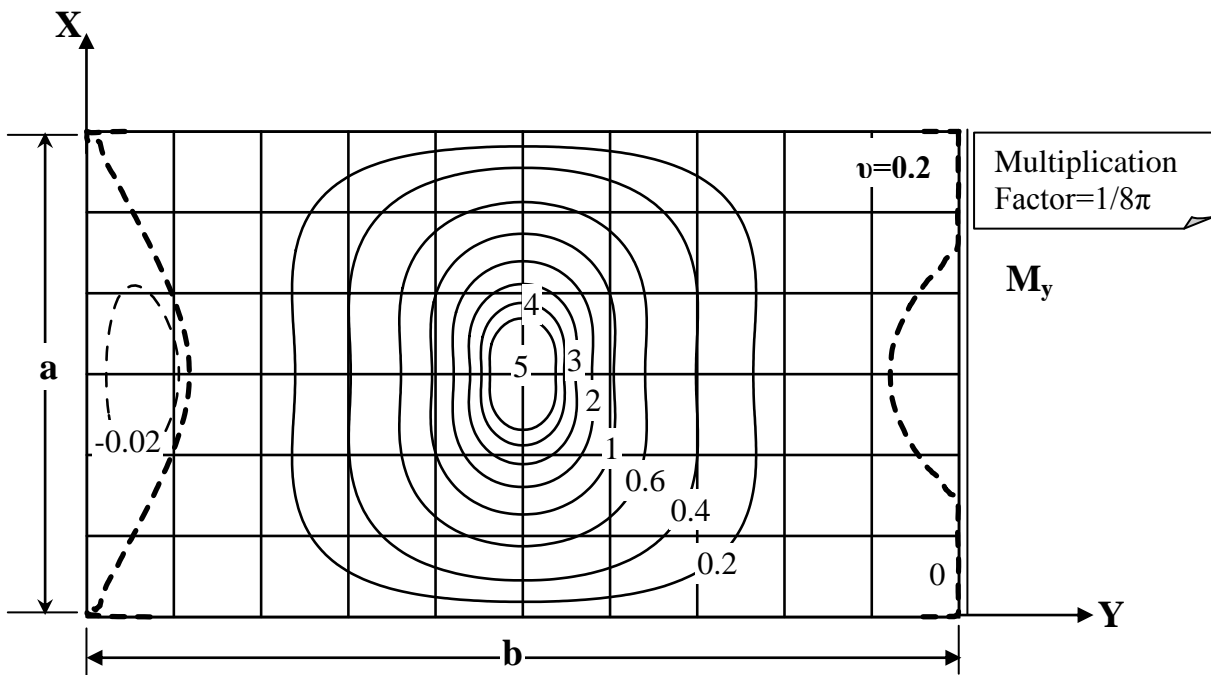
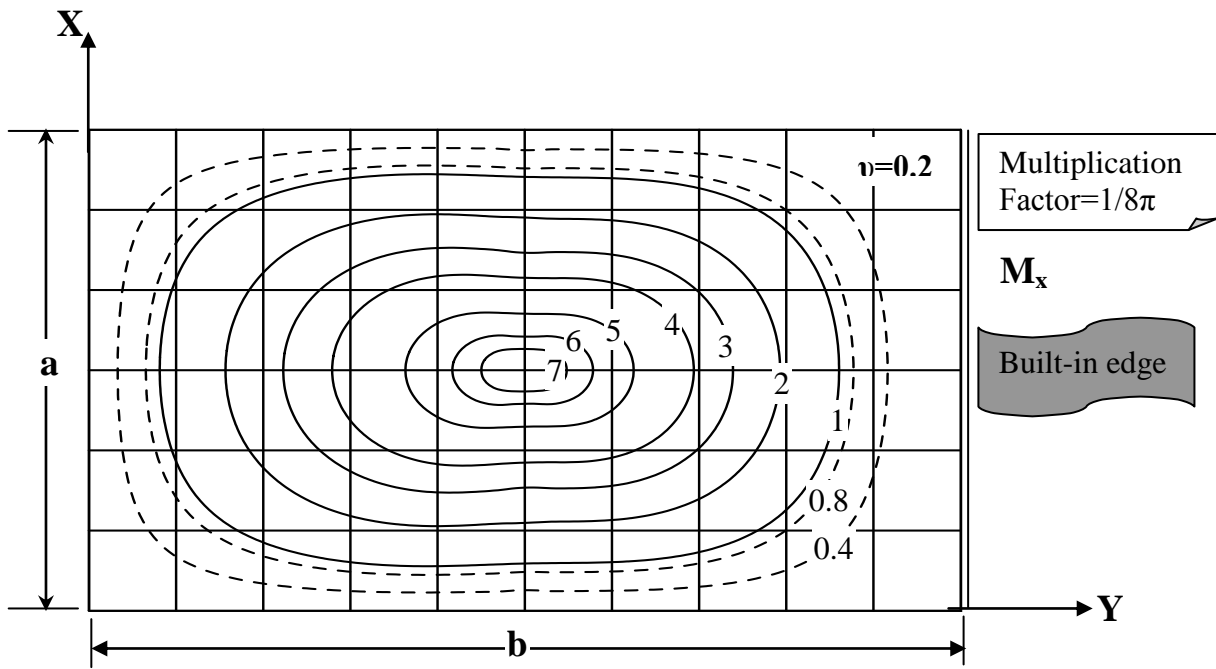


Fig.7 influence surface for m_x and m_y at the center of a rectangular plate ($a/b=0.6$) for Poisson's ratio of 0.2.

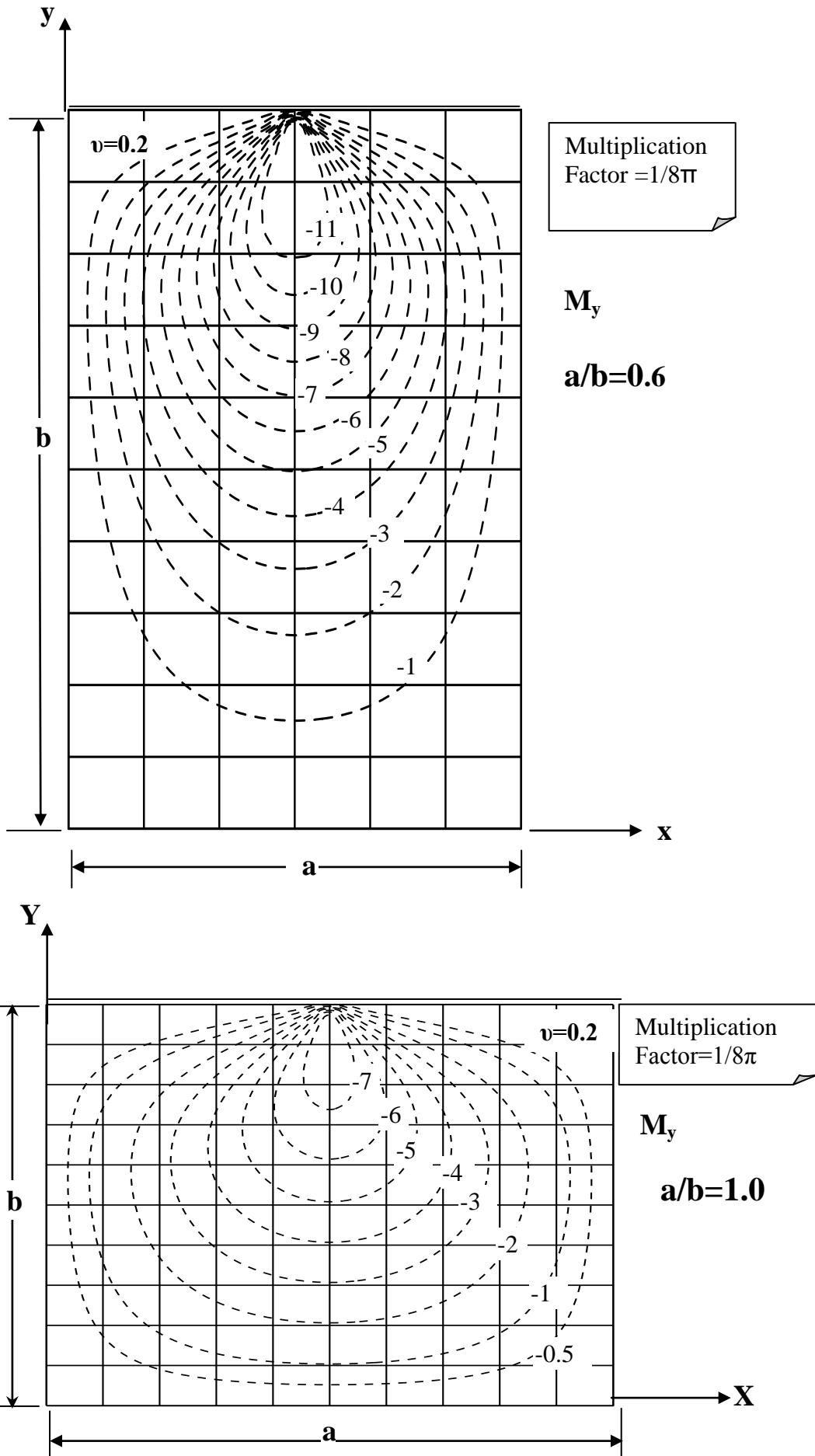


Fig.8 influence surface for m_y at the center of built-in edge of a rectangular plate ($a/b=0.6$ and $a/b=1.0$) for Poisson's ratio of 0.2.4808

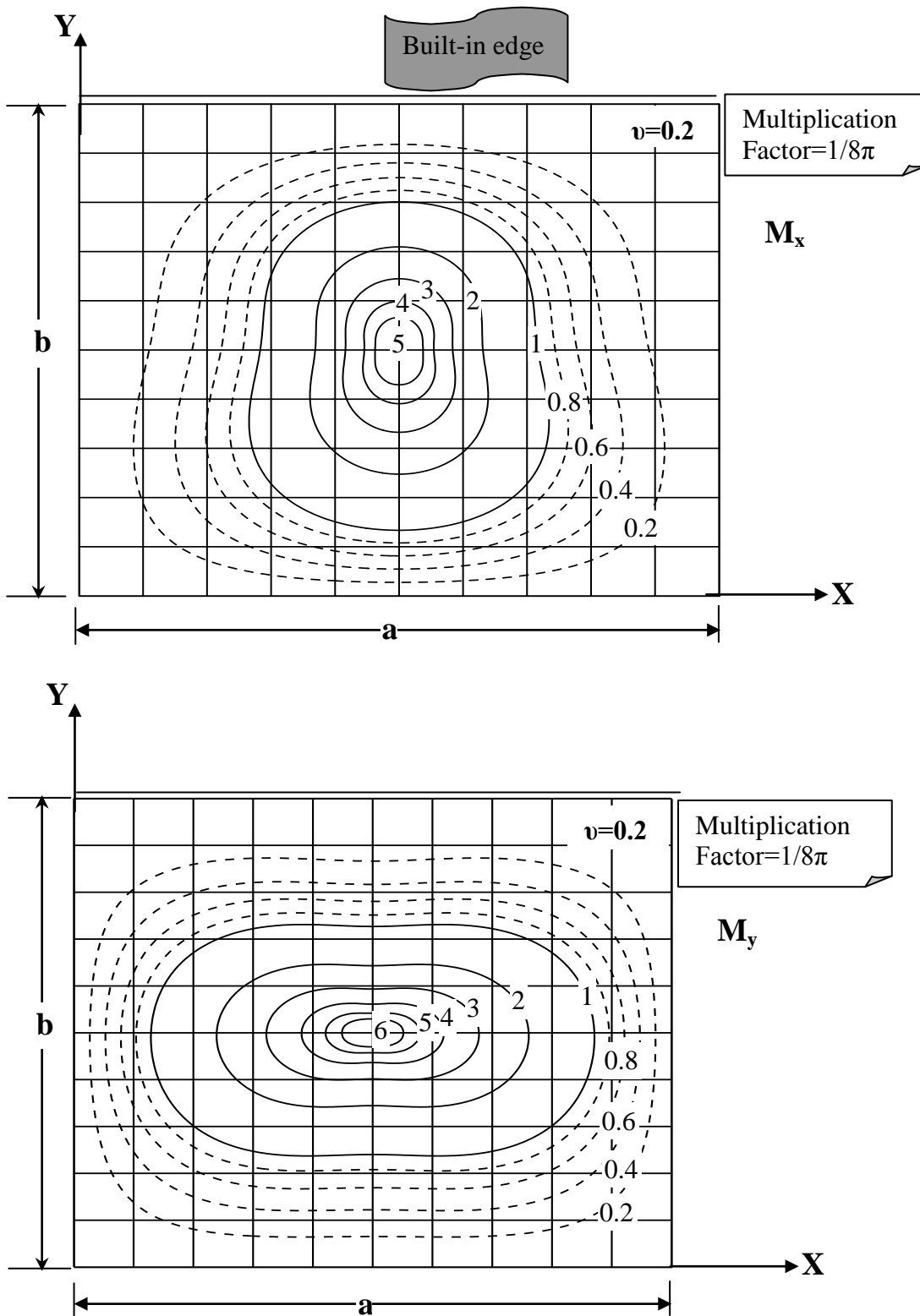


Fig.9 influence surface for m_x and m_y at the center of a rectangular plate ($a/b=1.0$) for Poisson's ratio of 0.2.

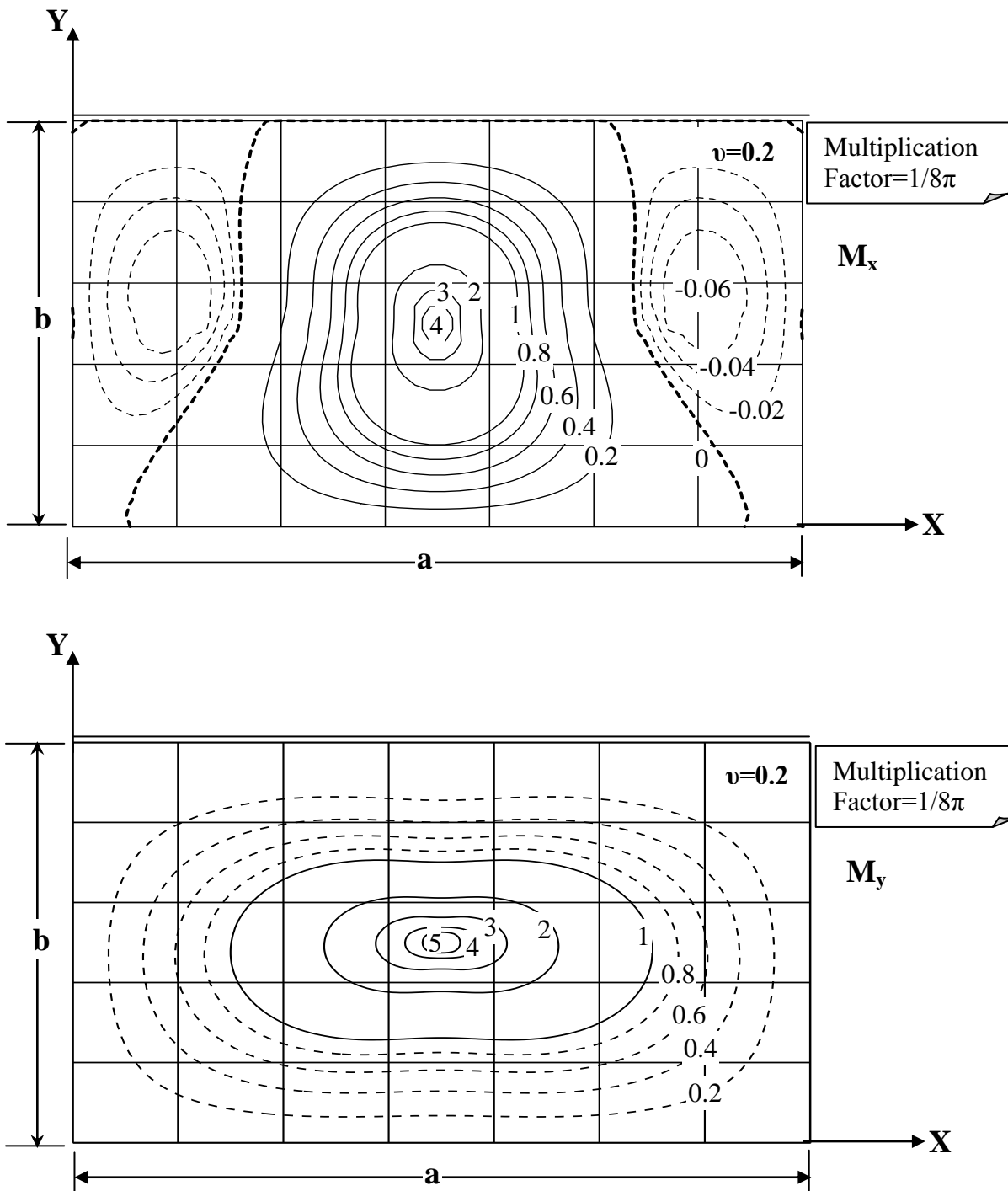


Fig.10 influence surface for m_x and m_y at the center of a rectangular plate ($a/b=1.4$) for Poisson's ratio of 0.2.

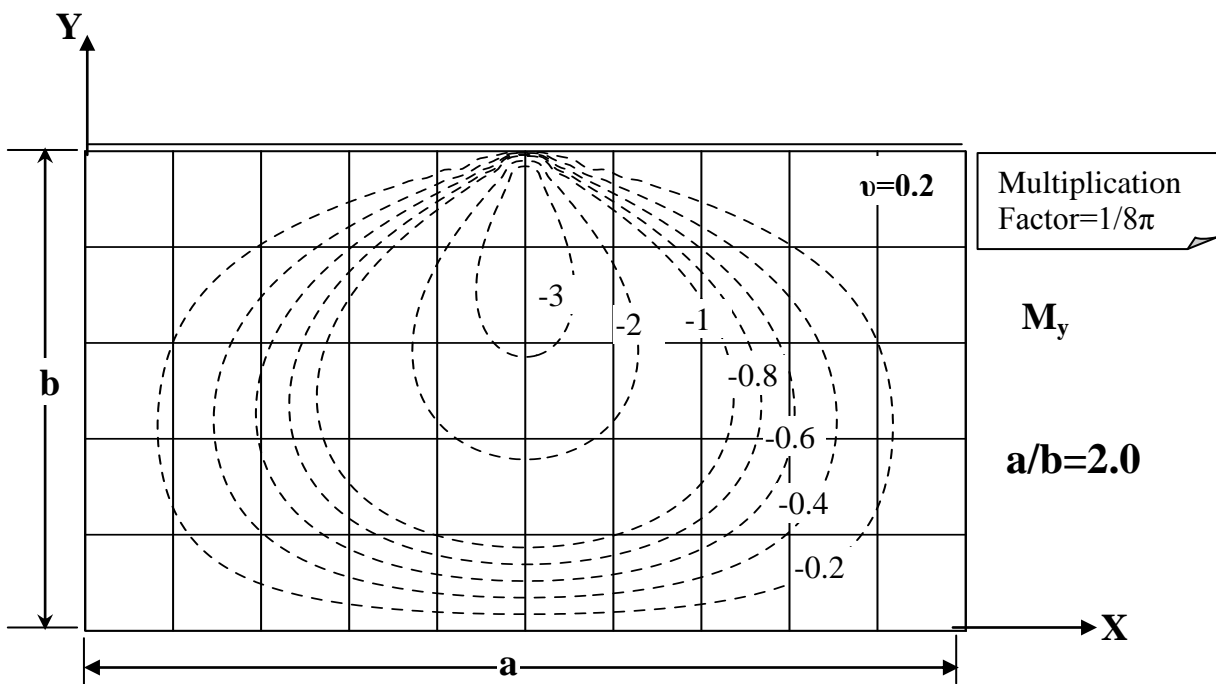
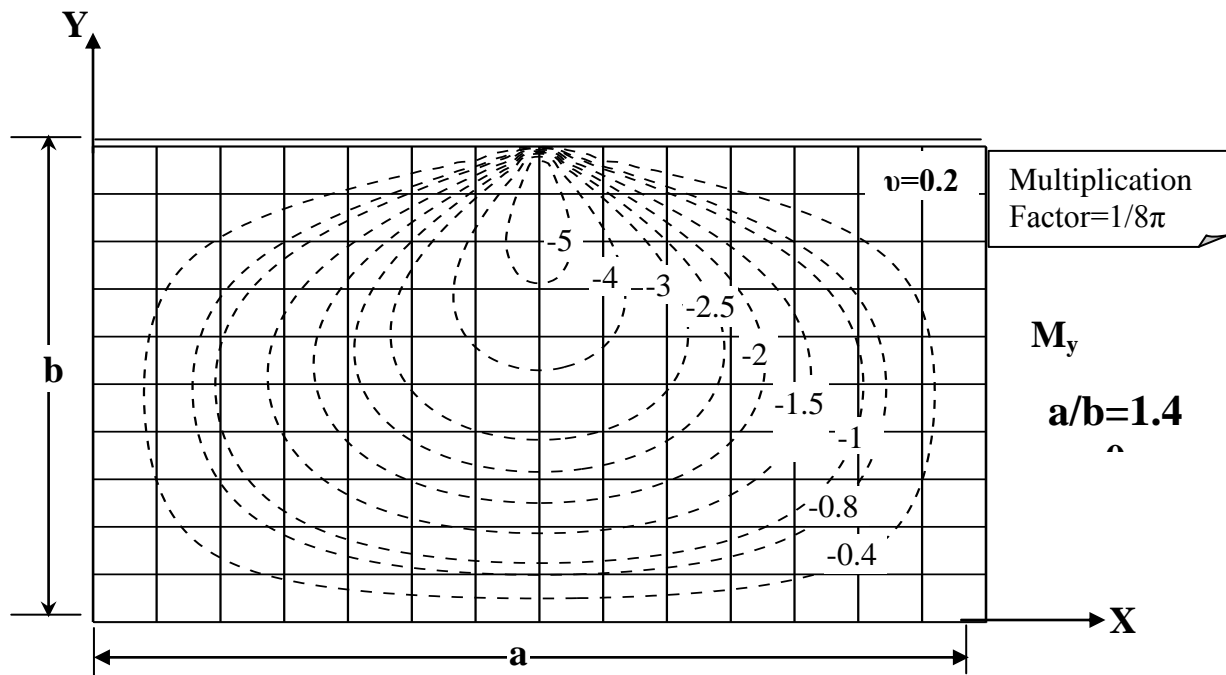


Fig.12 influence surface for m_y at the center of built-in edge of a rectangular plate ($a/b=1.4$ and 2.0) for Poisson's ratio of 0.2 .

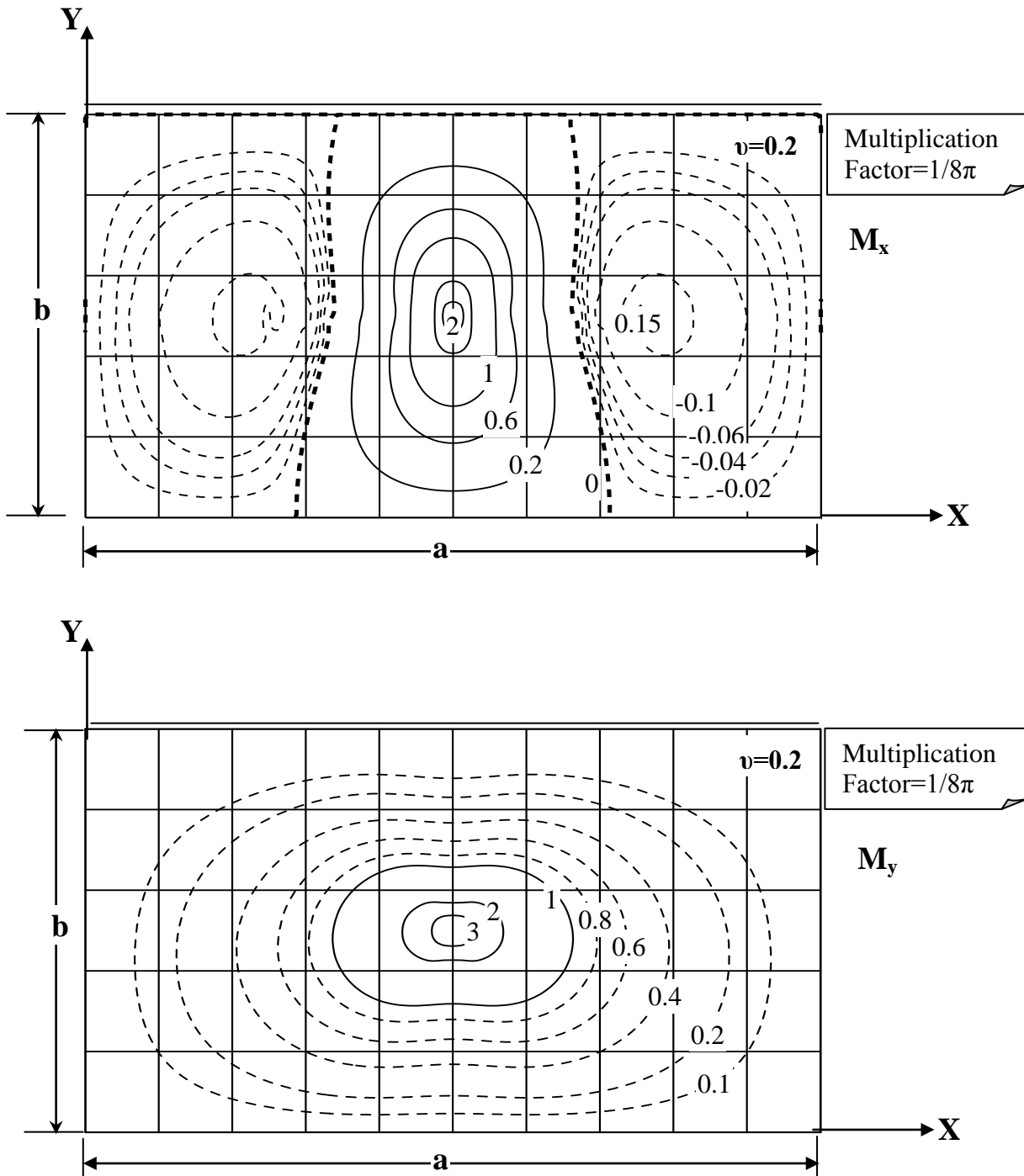


Fig.13 influence surface for m_x and m_y at the center of a rectangular plate ($a/b=2.0$) for Poisson's ratio of 0.2.

It is observed from figure 9 that for the case of square plates the influence surfaces for both m_x and m_y are represented by positive contour lines only. The influence surfaces for m_x at the center of the rectangular plates for aspect ratio of 1.4 and 2.0, are represented by negative and Positive contour lines while those for m_y are represented by positive contour lines as shown in figures 11 to 12. For rectangular plates with aspect ratio smaller than 1.0, such as 0.6, the influence surfaces for both the m_x and m_y at the center of the plate are represented by positive contour lines as shown in figure 7. All influence surfaces for bending moment m_y at the center of built-in edge for rectangular plates having aspect ratio ranging from 0.6 to 2.0, are represented by negative contour lines as shown in figures 7-10-13. For partial loading, there is a possibility for negative bending moment m_x at the center of the plate which increases as the aspect ratio increases.

APPLICATIONS:

To show how the influence surfaces can be used not only for concentrated loads but also for line and strip loads, the following applications are presented.

EVALUATION OF THE BENDING MOMENT M_x DUE TO A LINE LOAD:

For the case of a rectangular plate simply supported at three edges and built-in at the fourth edge with aspect ratio $a/b=1.4$ and a Poisson's ratio of 0.2 subjected to a line load extending in the x -direction as shown in Figure 14, the evaluation of the bending moment M_x at the center of the plate can be achieved by using the corresponding influence surface as follows:

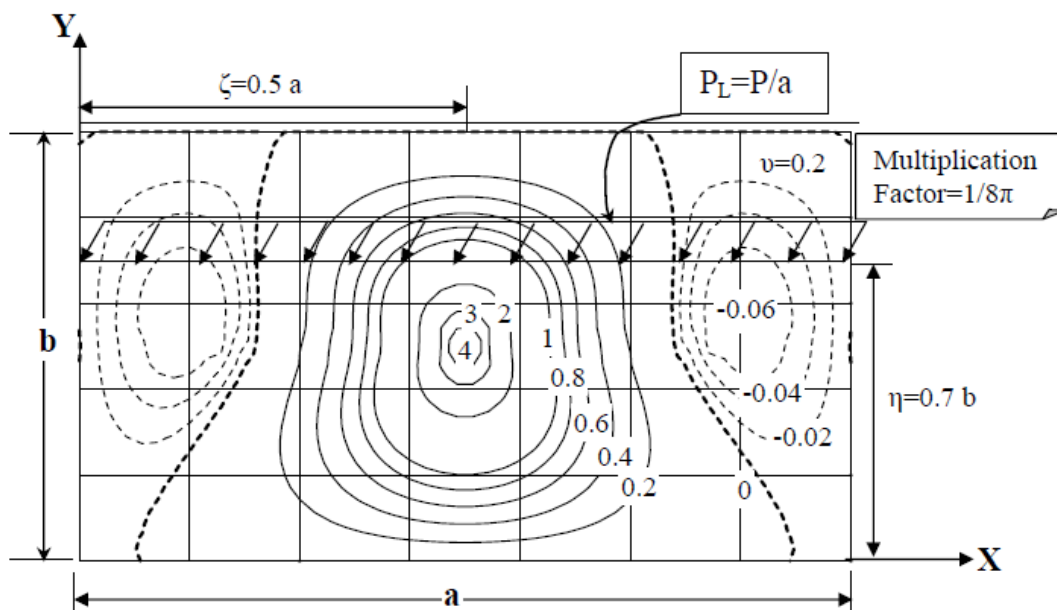


Fig.14 influence surface for m_x of a rectangular plate having an aspect ratio of 1.4 and a Poisson's ratio of 0.2 subjected to a line load extending in the x -direction at $\eta=0.7b$.

According to **Pucher(1973)**, the bending moment **M_x** produced at the observation point (x, y) due to a line load can be calculated from this formula

$$(M_x)_{(x,y)} = \int_s p(s) \cdot \bar{X}(x, y) \cdot ds \tag{19}$$

where

x and y= coordinates of the observation point.

p(s) is the line load intensity.

$\bar{X}(x, y)$ are the influence values of the bending moment corresponding to applied line load.

The integration in Eq.(19) represents the area integral of the influence values over the loaded line which can be computed by using the Simpson's rule (**Saffand Snider, 2000**) as follows

$$\int_a^b f(x) \cdot dx = \frac{h}{3} \sum_{k=1}^n \{f(x_{2k-2}) + 4f(x_{2k-1}) + f(x_{2k})\} \tag{20}$$

where

$h=b-a/2n$ is the distance between any two points of the partition.

$f(x_0), f(x_1), f(x_2), \dots, f(x_{2n})$ are the functions of defined integral at the points $x_0, x_1, x_2, \dots, x_{2n}$ respectively.

$2n$ =the number of equal parts of divided interval (a, b).

Because the influence surface for **m_x** is symmetric about the y-direction through the center of the plate as shown in Figure (14), only one half of the corresponding influence values for **m_x** are represented in Figure.(15).

The ordinates of the influence surface for **m_x** in Figure (14) are dimensionless, therefore the area in Figure.(15) is obtained as a dimensionless quantity by applying the Simpson's rule on the influence values of **m_x** .

Note that in Figure.(15), the influence values corresponding to line load are obtained from the influence surface at the interval of $\Delta(x/a)=0.05$.

This area becomes $F=0.152$ and the dimensionless bending moment **m_x** can be computed as follows:

$$m_x = 2 \cdot F \cdot \text{multiplication factor} = 2 \cdot 0.152 \cdot (1/8\pi) = 0.012$$

According to Eq.(11) the bending moment **M_x** at the plate center evaluated by using the influence surface becomes

$$M_x = \frac{m_x P_L a^2}{b} = 0.012 \frac{P_L a^2}{b} \tag{21}$$

The bending moment M_x at the plate center was calculated also using the computer program (EBM) which gave

$$M_x = \frac{m_x P_L a^2}{b} = 0.0125 \frac{P_L a^2}{b} \tag{22}$$

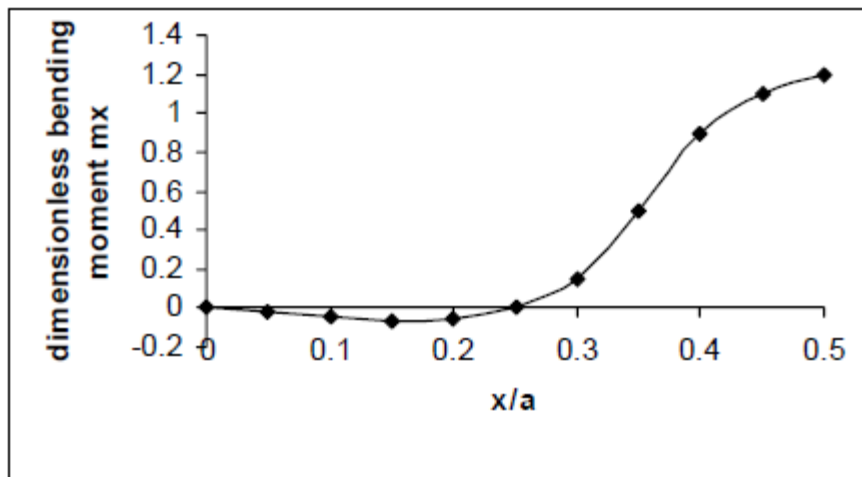


Fig.(15) variation of the bending moment m_x at the center of a rectangular plate with $a/b=1.4$ and a Poisson’s ratio of 0.2 corresponding to a line load extending in the x -direction at a distance $\eta=0.7b$ in the y -direction.

The small difference in the results is due to the interpolation of m_x resulting from the influence surface at the chosen interval.

EVALUATION OF THE BENDING MOMENT M_y DUE TO A STRIP LOAD:

For the case of a rectangular plate simply supported at three edges and built-in at the fourth edge with aspect ratio $a/b=1.4$ and a Poisson’s ratio of 0.2 subjected to a strip load extending in the y -direction at a distance of $\zeta=0.8a$ in the x -direction as shown in Fig.(16) , the evaluation of the bending moment M_y at the center of the plate can be achieved by using the corresponding influence surface shown in Fig.(17)

According to **Pucher(1973)**, the bending moment M_y produced at the observation point (x, y) due to a distributed load can be calculated from this formula

$$(M_y)_{(x,y)} = \iint_A p(\xi, \eta) \bar{X}(x, y; \xi, \eta) . dx dy \tag{23}$$

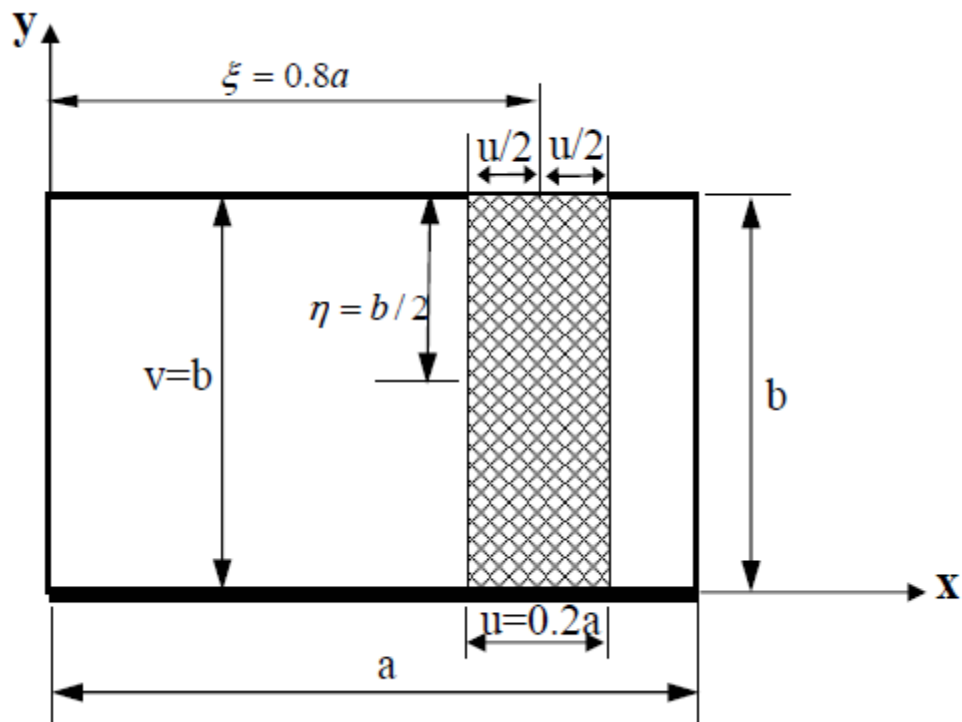


Fig.(16) rectangular plate with aspect ratio of 1.4 and having a Poisson's ratio of 0.2 subjected to a strip load in the y-direction.

Where

$\bar{X}(x, y; \xi, \eta)$ are the influence values of the bending moment corresponding to the applied distributed load.

$p(\zeta, \eta)$ is the distributed load.

To evaluate the double integral of this formula, a strip load is plotted into the influence surface for **my** and the area under this load is divided into five sections perpendicular to the x-direction of the plate as shown in Figure (17).

The evaluation of the individual areas is made by plotting the shape of the different sections separately as shown in Figure (18). Note that a uniform interval $\Delta(y/b)=0.05$ was used and the corresponding **my** - values were interpolated from the corresponding influence surface.

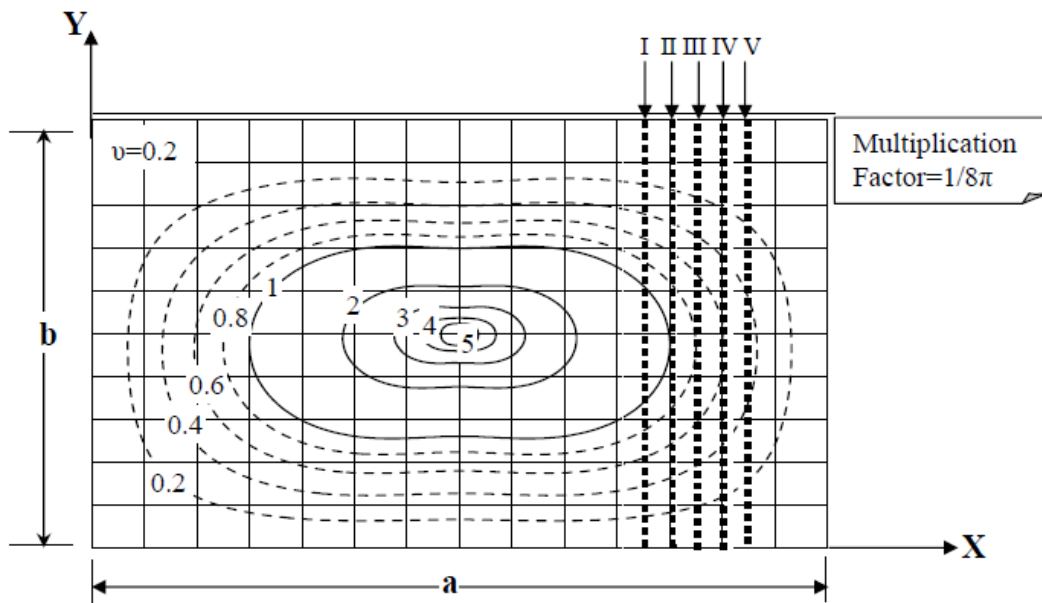


Fig.(17) influence surface for m_y at the center of a rectangular plate ($a/b=1.4$) for Poisson's ratio of 0.2 subjected to a strip load in the y-direction.

Thus, the individual areas are computed by using Simpson's rule as discussed before and the following results are obtained

$$F_I=0.541, F_{II}=0.431, F_{III}=0.348, F_{IV}=0.301, F_V=0.22$$

The spacing between the individual sections $\Delta(u/a)=0.05$ and the multiplication factor is $1/8\pi$. Thus, using Simpson's one third rule again, the dimensionless bending moment m_y becomes

$$m_y = 1/3 * 0.05 * (1/8\pi) * F_I + 4F_{II} + 2F_{III} + 4F_{IV} + F_V = 0.003$$

According to Eq.(12) the bending moment M_y at the plate center becomes

$$M_y = m_y q_0 a^2 = 0.003 q_0 a^2 \tag{24}$$

The bending moment M_x at the plate center was evaluated also using the computer program (EBM) which gave

$$M_y = 0.0031 q_0 a^2 \tag{25}$$

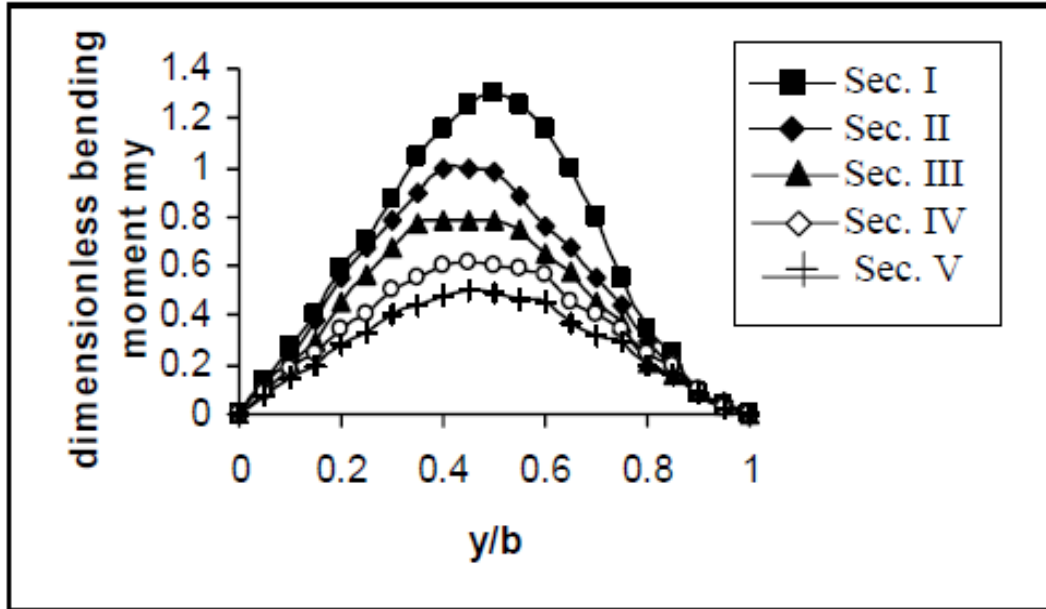


Fig.(18) the distribution of the bending moment m_y at the center of a rectangular plate with aspect ratio $a/b=1.4$ and a Poisson's ratio of 0.2 corresponding to a strip load extending in the y -direction and having $\zeta=0.8a$

This result is in excellent agreement with that obtained using the influence chart. It can be concluded from these applications that for practical purposes, the use of influence surfaces to evaluate the bending moments due to various cases of loading provides very satisfactory results which are in excellent agreement with those obtained using the computer program (EBM). To achieve higher accuracy with saving in time, the computer program (EBM) written in this work is strongly recommended.

CONCLUSIONS:

- There is good agreement between the developed analytical solution with that presented by **Timoshenko and Woinowsky-Krieger (1989)** for the case of a rectangular plate with aspect ratio $a/b=1.2$ and Poisson's ratio equal to 0.2 under the effect of uniform strip load.
- There is good agreement between the developed influence surface in this work with those presented by **Pucher (1973)** for the case of a square plate ($a/b=1.0$) having a Poisson's ratio equal to zero with the observation point at the center of the plate.



- The negative regions of influence surfaces for bending moment m_x at the center of the plate increase as the aspect ratio increases while those for m_y decrease with increasing aspect ratio.

REFERENCES

- ACI Committee 363, (1984), "**State of the Art Report on High-Strength Concrete** ", Journal of ACI, Vol.81, No.4-6, pp 383-384.
- Boyd, SK., Ronsky, JL., Lichti, DD., Salkauskas, D. and Chapman, MA. , (1999), "**Joint Surface Modeling With Thin- Plate Splines** " ASME, 121,pp 525-532.
- Cusens, A.R. and Pama, R.P., (1975), "**Bridge Deck Analysis** ", John Wiley and Sons.Inc., London-New York, Sydney, Toronto.
- Darwing , D and Pecknold, D. A., (1977), "**Nonlinear biaxial stress for concrete**" , ASCE, Engineering Mechanics Journal , Vol.103, EM.4, pp 229-241.
- Francis, A.; Bordette, E.G. and Deatherage, J.H., (1991), "**Elastic Modulus, Poisson's ratio, and Compressive Strength Relationships at Early ages** ", Journal of ACI, Vol.88, No.1, Jan, pp 3-10.
- Hambly, E.C,(1976), " **Bridge Deck Behaviour** ", Chapman and Hall, London- New York.
- Girkmann, K., (1963), "**Flaechentragwerke**" **Sechste Auflage Springer-Verlag Wien**
- Klink, S., (1985), "**Actual Poisson's Ratio of Concrete** ", Journal of ACI, Vol.82, No.5-6, pp813- 817.
- McCormac, J.C., (1989), "**Structural Steel Design** ", Harper and Row Publishers, New York,London, Sydney, Tokyo.
- Merritt, F.S., (1999), "**Structural Steel Designer's Handbook** ", Third Edition, McGraw-Hill , Inc.
- Mirza , S.A. , Hatzinivdas, M. and Mcgreger , J.C., (1979), "**Statistical description of strength of oncrete**" ASCE, Engineering Mechanics Journal, Vol.105, ST.6, pp 1021-1037.
- Razouki, S.S and Karim, B.H., (2005), "**Effect of Poisson's ratio on the Bending Moment Influence Surfaces for Simply Supported Rectangular Plates** ", Engineering Journal of the University of Qatar, Vol.18, pp. 67-92.
- Razouki, S.S and AL-Ani, S.H. (2009), "Bending moment influence surfaces for rectangular concrete slabs simply supported at two parallel edges and built-in at the others", paper accepted for publication in Engineering and Development Journal Al- Mustansiriya University, Baghdad.

- Kupfer, H.B. and Gerstle, H. (1973), "**Behavior of concrete under biaxial stress**" ASCE, Engineering Mechanics Journal, Vol.99, EM.4, pp 853-866.
- LARSA, (2006), "**Influence Line and Surface Analysis** " Email: info@Larsa4D.com
- Pucher, E.,(1973), " **Influence Surfaces of Elastic Plates** ", Fourth Edition, Springer-Verlag Wien, New York.
- Selvadurai, A.P.S, (1979), "**Elastic analysis of soil Foundation interaction** ", Elsevier Scientific Publishing Company,Amsterdam, Oxford, New York .
- Szilard, R., (1974), " **Theory and Analysis of Plates: Classical and Numerical Methods** ", Prentice-Hall Inc, Englewood, Cliffs, New Jersey.
- Taylor, R. L. and Govindjee S., (2004) "**Solution of Clamped Rectangular Plate Problems**" Structural Engineering Mechanics and Materials, Communi. Numer. Meth. Eng. 20, pp 757-765.
- Timoshenko, S.P and Woinowsky-Krieger, S., (1989), "**Theory of Plates and Shells** ", Second Edition, McGraw-Hill Book Company, New York, pp 79-198.
- Wang,HC., Ryu ,J. and Han, JS.,(2000), "**A New Method for the Representation of Articular Surfaces Using the Influence Surface Theory of Plates** " J Biomech, 33, pp 629-633.
- Zehnder, A. T., Hui, C. Y. and Potdar, Y., (1998), "**Fracture Mechanics of Thin, Cracked Plates Under Tension, Bending and Out-Of-Plane Shear Loading**" Proceedings of the Second joint NASA/FAA/DoD Conference on Aging Aircraft, (C. Harris, ed.), 33,pp. 627-634.



NOTATIONS

Symbol	Definition
a	Length of the built-in edge
a_{mn}	Coefficients of a double Fourier sine expansion of any kind of loading $q(x, y)$
b	The dimension of the plate perpendicular to built-in edge
D	Flexural rigidity of the plate
E	Modulus of elasticity
E_m	Coefficient of a single sine Fourier series of distributed moment M_y at the built-in edge
h	Plate thickness
m and n	Integers 1,2,3,..... of the double Fourier series
M_x	Bending moment per unit length acting on the edges parallel to the y-axis
M_y	Bending moment per unit length acting on the edges parallel to the x-axis
M_{xy}, M_{yx}	Twisting moment per unit length of sections perpendicular to the x and y axes respectively
m_x and m_y	Dimensionless bending moments
p	Concentrated load
q	Lateral load (load per unit area)
q_0	Intensity of the uniformly distributed load
u and v	The sides of the rectangular loaded area parallel to the x and y- axes respectively
$w(x, y)$	Deflection surface
x and y	Cartesian coordinates of the observation point
η	y-coordinate of the centroid of the load
υ	Poisson's ratio
ζ	x-coordinate of the centroid of the load